4. Robello, D. R.; Moore, J. A. *Macromolecules* **1989**, *22*, 1084.
5. Robello, D. R.; Moore, J. A. *Macromolecules* **1986**, *19*, 2667.
6. Mehta, P. G.; Moore, J. A. *Macromolecules* **1993**, *26*, 916.
7. Mehta, P. G.; Moore, J. A. *Polym. Mater. Sci. Eng.* **1990**, *63*, 351.
8. Kim, S. Y.; Mehta, P. G.; Moore, J. A. *Macromolecules* **1994**, *26*, 3504.
9. Kim, J. H.; Moore, J. A. *Korea Polym. J.* **1993**, *1*, 161.
10. Gong, M. S.; Kim, S. T.; Lee, J. O.; Kim, Y. S. *Polymer (Korea)*, **1991**, *15*, 95.
11. Gong, M. S.; Kim, S. T.; Moon, H. S. *Makromol, Chem. Rapid Commun.* **1991**, *12*, 591.
12. Gong, M. S.; Moon, H. S.; Kim, J. S.; Kim, C. B. *Polym. J.* **1993**, *25*, 193.
13. Gong, M. S.; Kim, T. M.; Shin, J. C. *Macromolecules* in press.
14. Gong, M. S.; Kim, J. S.; Kim, S. T.; Choi, S. H. *Polymer J.* **1993**, *25*, 763.
15. Gong, M. S.; Kim, S. T.; Moon, H. S. *Macromolecules* **1992**, *25*, 7392.
16. Gong, M. S.; Moon, S. H.; Kim, J. B.; Lee, S. J. *Bull. Korean Chem. Soc.* **1994**, *15*, 1089.
17. Gong, M. S.; Cho, H. G.; Choi, S. H.; Kim, B. G. *Macromolecules* **1993**, *26*, 6654.
18. Gong, M. S.; Kim, Y. S.; Kim, B. G. *Polym. J.* **1994**, *26*, 1910.
19. Dean, J. A. *Lange Handbook of Chemistry*; 13th Ed. McGraw Hill, 1985, 5-18~60.
20. Gong, M. S.; Kim, T. M.; Moon, S. H.; Kim, S. G. *Bull. Korean Chem. Soc.* **1994**, *15*, 901.
21. Adams, R.; Bullock, J. E.; Wilson, W. C. *J. Am. Chem. Soc.* **1923**, *45*, 521.
22. Hatt, H. H. *Org. Synth. II* **1943**, 395.
23. Stern, E. S.; Timmons, C. J. *Electronic Absorption Spectroscopy in Organic Chemistry*; 3rd Ed.; Edward Anord LTD.: London 1976.

^{1}H NMR Estimation of Multi-Redox Potentials of Cytochrome c_3 from *Desulfovibrio vulgaris* Hildenborough

Jang-Su Park*, Shin Won Kang, and Sung Nak Choi

Department of Chemistry, College of Natural Sciences, Pusan National University, Pusan 609-735, Korea
Received December 20, 1994

The macroscopic and microscopic redox potentials of tetrahemoprotein, cytochrome c_3 from *Desulfovibrio vulgaris* (Hildenborough) (*Dv*H) were estimated from ^{1}H NMR and differential pulse polarography (DPP). Five sets of NMR resonances were confirmed by a redox titration. They represent cytochrome c_3 molecules in five macroscopic redox states. The electron transfer in cytochrome c_3 involves four consecutive one-electron steps. The saturation transfer method was used to determine the chemical shifts of eight heme methyl resonances in five different oxidation states. Thirty two microscopic redox potentials were estimated. The results showed the presence of a strong positive interaction between a pair of particular hemes. Comparing the results with those of *Desulfovibrio vulgaris* Miyazaki F (*Dv*MF), it was observed that the two proteins resemble each other in overall redox pattern, but there is small difference in the relative redox potentials of four hemes.

Introduction

Cytochrome c_3 isolated from the sulfate-reducing bacteria *Desulfovibrio vulgaris* Hildenborough (*Dv*H) is a tetraheme electron transfer protein which plays an impotant role in the metabolism of sulfur compounds and hydrogen.[1] It was independently identified by Postgate in England and Ishmoto in Japan in 1954.[2~7] Cytochrome c_3 has a molecular weight of approximately 13,000 with 107 amino acid residues in a single polypeptide chain. The amino acid sequences of cytochrome c_3 show no homology with mammalian cytochrome *c* except for four sequences: two Cys-x-y-Cys-His, and two Cys-w-x-y-z- Cys-His which resemble the Cys-x-y-Cys-His sequences of cytochrome *c*. These four sequences provide thioether attachments of the heme to the polypeptide chain and the histidine ligand to the heme iron atom.[8]

Extensive investigations of cytochrome c_3 from several genera have been carried out. Amino acid sequences of cytochrome c_3 from *Desulfovibrio vulgaris*, Miyazaki F (*Dv*MF), *Desulfovibrio vulgaris* Hildenborough (*Dv*H), *D. gigas, D. salexigens, D. desulfuricans* and *D. desulfuricans Norway* (*DdN*) have been determined.[9] Comparisons of their primary structures show rather poor homology among the six cytochromes c_3 above. The closest pair is *Dv*H and *Dv*MF. They differ by 14 out of 107 amino acid residues.[9] The complete three dimensional structures of *Dv*MF and *Dv*H have been obtained.[10~12]

The redox potential of cytochrome c_3 is an important parameter in understanding its physiological role.

Since cytochrome c_3 has four redox centers, four macro-

*To whom correspondences should be addressed.

scopic formal redox potentials and thirty-two microscopic formal redox potentials ("formal" is deleted hereafter for simplicity) can be defined.[13,14] Many efforts have been made to determine its macroscopic redox potentials[15~18] and microscopic redox potentials.[13,14,19~22] The macroscopic redox potentials of cytochrome c_3 from *Dv*MF were determined by means of electrochemical methods (potentiometry and differential pulse polarography)[17] and NMR.[18] And the thirty-two microscopic redox potentials of this protein were estimated with the combined use of the macroscopic redox potentials with the electron distribution probabilities obtained from the chemical shift values of NMR signals.[14] Although analysis of the microscopic redox potentials of *Dv*MF cytochrome c_3 by EPR has also been reported,[22] the resolution of EPR spectra was not satisfactory for conclusive analysis. The assignment of the microscopic redox potentials to the hemes in the crystal structure has been performed recently by means of NMR.[23] Such correlation has also been reported for cytochrome c_3 from *Dd*N[24] and *Dv*H.[25,26]

It is very interesting to compare the redox processes of two cytochrome c_3 from two different strains, *Dv*MF and *Dv*H. Especially, the understanding of the influence of their structural differences on the interheme interaction is of importance. The aim of the present study is to obtain the microscopic redox potentials of cytochrome c_3 from Hildenborough strain by using ^{1}H NMR and differential pulse polarography (DPP).

Materials and Methods

Desulfovibrio vulgaris Hildenborough was cultured in medium C[L]. Cytochrome c_3 was purified according to the procedure reported previously.[27] The purity index (A_{552}(red)/A_{280} (ox)) of the final sample was over 3.0. The purity was confirmed also by SDS-polyacrylamide gel electrophoresis. In NMR experiments, a trace amount of hydrogenase was added to a 1.3 mM cytochrome c_3 solution (molar ratio of *ca.* 0.001) as a redox catalyst. The hydrogenase was extracted from *D. vulgaris* Miyazaki F. and purified as reported elswhere.[28] Partial reduction (refered to as an intermediate redox stage hereafter) of a cytochrome c_3 solution was achived by controlling the partial pressure of hydrogen and argon gases in an NMR tube.

^{1}H NMR spectra were obtained on a Brucker AM 400 MHz spectrometer, Yokohama National University, at 30 ℃ in a 30 mM phosphate buffer (p^{2}H 7.0). Chemical shifts are presented in parts per million relative to the internal standard of 2,2-dimethyl-2-silapentane-5-sulfonate (DSS). Saturation transfer experiments were carried out for various intermediate redox stages in order to assign heme methyl resonances in the five macroscopic oxidation states. Sixteen free induction decays (FID) were accumulated repeatedly under on-resonance and off-resonance irradiation for 1s. The irradiation was adjusted to supress the signal intensity to half the original one. One thousand transients were accumulated for each FID. Differential pulse polarograms (DPP) were measured at a dropping mercury electrode with a potentiostat, Fuso polarograph Model 312. Modulation amplitude, sweep rate, drop time, and sampling time were 10 mV, 2 mVs^{-1}, 2 s, and 20 ms, respectively.

Potentials referring to the silver/silver chloride reference electrode in saturated potassium chloride at 30 ℃ were presented in this work.

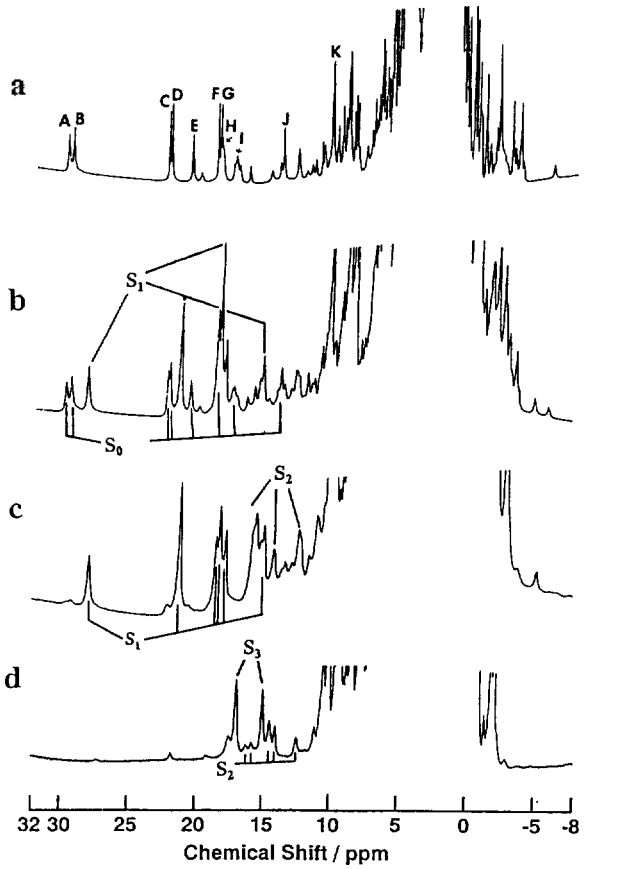

Figure 1. 400-MHz ^{1}H NMR spectra of cytochrome c_3 from *D. vulgaris* Hildenborough, in a variety of redox stages at 30 ℃. The stage of oxidation was changed from the fully oxidized (a) to the intermediate reduced states (b, c and d) by changing the hydrogen partial pressure in the presence of hydrogenase. The heme methyl signals are labeled on top. S_i is the macroscopic oxidation state for the i-th redox process.

Results and Discussion

Assignments of heme methyl resonances. The ^{1}H NMR spectrum of the fully oxidized cytochrome c_3 is presented at Figure 1a.

Signals at low field with three proton intensity were assigned to heme methyl groups. These are designated as A, B, C··· from the low field end. It was possible to assign 11 out of 16 heme heme methyl resonances. This spectrum is similar to that reported previously.[27,29] Figure 1 shows cytochrome c_3 in various oxidation stages proceeding from the oxidized to the reduced form. As reduction progressed, signals at low field decresed and new signals appeared at higher field which then subsequently disappeared again. Three sets (S_1, S_2 and S_3) of such signals were also observed on reoxidation of cytochrome c_3. It turned out that the intermolecular electron exchange rate of *Dv*H cytochrome c_3 is slower and intramolecular one is faster than the NMR time scale in the redox process.

Saturation-transfer experiments were carried out to deter-

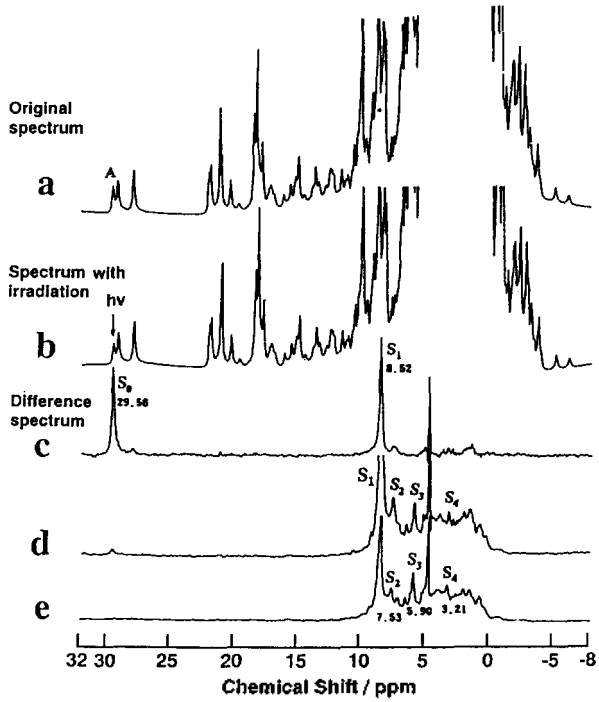

Figure 2. 400-MHz Saturation transfer measurement to track the change of chemical shift of heme methyl signal A. The signals at 29.56, 8.52, and 8.52 ppm were irradiated with the coexistence of S_0 and S_1 (c), S_0, S_1, S_2, S_3 and S_4 (d), and S_1, S_2, S_3 and S_4 (e), respectively. (a) and (b) are the off- and on-resonance normal spectra of (c), respectively.

mine the chemical shifts of the heme methyl groups in the five macroscopic oxidation states. Typically, the irradiation at the heme methyl proton of signal A shown in Figure 2 was carried out in the coexistence of the molecules belonging to S_0 and S_1

Its normal and saturation-transfer difference spectra are presented in parts (a, b) and (c), respectively, of Figure 2. The difference spectrum clearly shows that the chemical shift of methyl proton A in the S_1 state is 8.52 ppm. Then the methyl proton at 8.52 ppm was irradiated with the coexistence of the S_1, S_2, S_3 and S_4 states. The difference spectrum in Figure 2d and 2e shows that the chemical shift of heme methyl A in the coexistence of the S_1, S_2, S_3, and S_4 states. The signals of heme methyl A in S_2, S_3 and S_4 appeared at 7.53, 5.90 and 3.21 ppm, respectively.

This experiment was carried out on eleven heme methyl resonances. The results are summarized in Table 1.

A total of eight out of sixteen heme methyl resonances have been assigned to the five oxidation states. In the analysis of chemical shifts of *D. gigas*,[13] extrinsic pseudocontact shifts from the adjacent hemes were neglected. Chemical shifts of heme methyl groups are dominated by the intrinsic shift which depends strongly on the oxidation state of a single heme. This assumption is also reasonable for *Dv*H because pseudocontact shifts are inversely proportional to the 6th power of the distance. Following this assumption, the electron distribution probability (R) can be calculated from the chemical shifts of the five oxidation states. Table 2 gives the results obtained from eight methyl signals.

Table 1. Chemical shift (ppm) of heme methyl signals in the five macroscopic oxidation states at p^2H 7.0 and 30 ℃ in a 30 mM phosphate buffer

Signals	Oxidation states					
	S_0	S_1	S_2	S_3	S_4	ppm
A	29.56	8.52	7.53	5.90	3.21	
B	29.20	27.94	15.62	4.70	3.28	
C	22.09	21.16	15.79	4.63	3.20	
D	21.92	21.13	15.51	4.55	3.12	
E	20.38	18.43	14.20	15.69	3.43	
F	18.46	17.77	11.16	4.15	2.80	
G	18.25	17.76	11.14	4.16	2.82	
H	18.12	6.47	5.81	5.22	–	
I	17.09	5.65	5.24	–	–	
J	13.64	14.94	12.37	14.16	4.30	
K	10.11	5.46	–	–	–	

Table 2. Electron-distribution probability ($R_i^j=(\nu(S_{j-1})-\nu(S_j))/(\nu(S_0)-\nu(S_4))$) calculated from heme methyl chemical shifts at p^2H 7.0 and 30 ℃. By definition, R_i^j is the distribution probability at heme i of the electron introduced in the j-th reduction step. Eight methyl groups were classified into four hemes according to the largest R^j

Signals	R^I	R^{II}	R^{III}	R^{IV}	Heme
A	0.799	0.038	0.062	0.102	1
B	0.049	0.475	0.421	0.055	
F	0.044	0.422	0.448	0.086	2
G	0.032	0.429	0.452	0.087	
C	0.049	0.284	0.591	0.076	3
D	0.042	0.299	0.583	0.076	
E	0.115	0.250	−0.088	0.723	4
J	−0.139	0.275	−0.192	1.056	

Furthermore, eight heme methyl resonances were classified into four groups according to their largest R. In principle, heme methyl groups belonging to same heme should have the same electron distribution probability. However, R values for resonances related to the same heme determined here are scattered to a certain extent, suggesting that the extrinsic pseudocontact shifts are not negligible, thus inducing some error in the measurements. Nevertheless, some important conclusions can be deduced from Table 2. The electron transfer in each reduction step is actually delocalized among the four hemes. We can identify the site with the major electron distribution probability. Hemes 1, 2, 3 and 4 are reduced in consecutive steps.

Macroscopic and microscopic redox potentials. A tetraheme protein, such as cytochrome c_3 has five macroscopic oxidation states, S_0, S_1, S_2, S_3 and S_4 states, and four macroscopic formal potentials, $E_i^{\circ}(i=1\text{-}4)$, can be defined, as follows

$$E=E_i^{\circ}+(RT/F)\ln(f_{i-1}/f_i) \quad (1)$$

where E, R, F, T and f_i are the equilibrium potential, gas

Table 3. The electron-distribution probabilities of four hemes in the four reduction steps at p^2H 7.0 and 30 ℃ obtained by least-squares fitting

	R^I	R^{II}	R^{III}	R^{IV}	Standard deviation
Heme 1	0.789	0.030	0.061	0.110	0.0095
Heme 2	0.041	0.440	0.440	0.079	0.0064
Heme 3	0.046	0.288	0.587	0.080	0.0076
Heme 4	0.115	0.242	−0.088	0.731	0.0095

constant, Faraday constant, absolute temperature and mole fraction of cytochrome c_3 in the i-electron reduced states, respectively.

The macroscopic redox potentials, E_i^0, of *Dv*H cytochrome c_3 were determined by least-squares fitting of the differential pulse polarogram to the analytical equation for the four consecutive one-electron reversible electrode reactions,[15] which was confirmed to be the actual mechanism.[18] The results are: $E_1^0 = -457.4$ mV, $E_2^0 = -517.4$ mV, $E_3^0 = -535.0$ mV and $E_4^0 = -582.4$ mV (Ag/AgCl). E_i^0 represents the macroscopic redox potential for the i-th redox process (between S_{i-1} and S_i).

If one denotes each heme as o (for the oxidized form) or r (for the reduced form), the microscopic formal redox potentials of heme 1 (e_1), for example, can be defined as follows.

$$E = e_1^I + (RT/F)\ln([oooo]/[rooo]) \quad (2)$$

$$E = e_1^{II2} + (RT/F)\ln([oroo]/[rroo]) \quad (3)$$

$$E = e_1^{III23} + (RT/F)\ln([orro]/[rrro]) \quad (4)$$

$$E = e_1^{IV} + (RT/F)\ln([orrr]/[rrrr]) \quad (5)$$

where the superscript (II2, for example) stands for the reduction step (II) and the hemes remained reduced (heme 2). The concentration of the redox species with heme 2 reduced, for example, is given by [oroo]. The notation, e_1^{IV}, is the abbreviation of e_1^{IV234}. The theory regarding the analysis of the microscopic redox potentials was resented elsewhere.[14] In short, the microscopic redox potentials can be estimated by the use of the electron-distribution probabilities (R_i^j) and the macroscopic redox potentials, assuming the interaction potentials (I_{ij}). For example, R_1^I is the distribution probability at heme 1 of the electron introduced at the first reduction step, namely, $R_1^I = [rooo]/([rooo]+[oroo]+[ooro]+[ooor])$. The interacting potential, I_{ij}, can be defined as

$$I_{ij} = e_i^{IIj} - e_i^I = e_i^{IIIjk} - e_i^{IIk} = e_i^{IV} \text{ (or } e_i^{IVjkl}) - e_i^{IIIkl} \quad (6)$$

where i, j, k and l denote the heme numbering. It follows, for example, that

$$e_i^{IV} = e_i^I + I_{ij} + I_{ik} + I_{il} \quad (7)$$

The microscopic redox potentials were estimated.

Neglecting the contribution of the extrinsic paramagnetic shifts, the electron-distribution probability can be calculated from the observed chemical shifts, which are given in Table 3.

Here, heme methyl groups are classified to four hemes using the largest R_i^j at each reduction step, because methyl groups belonging to the same heme should have the same electron-distribution probability. The scattered values in Table 3 showed that the contribution of the extrinsic paramagnetic shifts is not negligible. The average electron-distribution probabilities were obtained by the least-squares method under the conditions of $\sum_j R_i^j = 1$ and $\sum_j R_i^j = 1$ for the data in Table 3.

The microscopic redox potentials at the first and fourth reduction steps, and the interacting potentials were calcula-

Table 4. The microscopic redox potentials (mV) at the first and fourth reduction step (e_i^I and e_i^{IV}, respectively), and interacting potentials (I_{ij})

Microscopic redox potentials (mV)		Interacting potentials (mV)	
e_1^I	−463.29	I_{12}	−7.7 (2.4)
e_2^I	−540.59	I_{13}	−24.6 (−30.6)
e_3^I	−538.12	I_{14}	−29.2 (−31.6)
e_4^I	−513.95	I_{23}	54.8 (43.6)
e_1^{IV}	−524.76	I_{24}	−22.5 (−20.0)
e_2^{IV}	−515.96	I_{34}	−8.5 (−8.1)
e_3^{IV}	−516.39		
e_4^{IV}	−574.23		

The vales in the parenthless are for cytochrome c_3 of *Dv*MF strain under the same conditions.

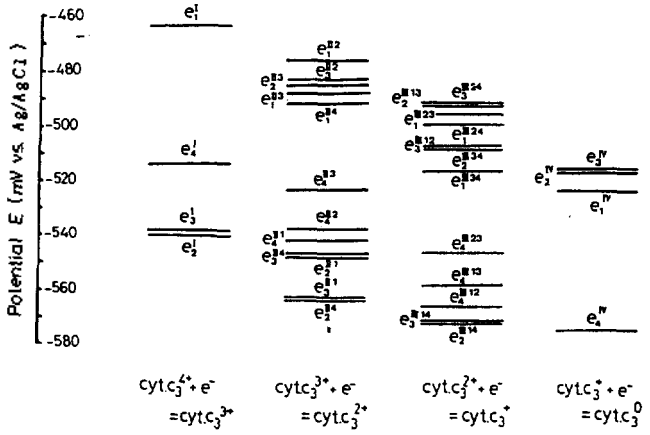

Figure 3. A diagram of thirty-two microscopic redox potentials of cytochrome c_3 estimated by NMR at 30 ℃. e_i denotes the microscopic redox potential of heme i. The superscript indicates the reduction step as in the case of the macroscopic redox potentials. I and IV show the first and fourth reduction step, respectively. A combination of step numbers (II, III) and heme numbers (1, 2, 3 and 4) was used in the superscript to described the microscopic redox potentials in the second and third reduction steps because of the multiple pathway. For example, *IIIjk* is the abbreviation of the third reduction step with reduced hemes j and k. According to this principle, the fourth reduction step also can be written as *IVjki*, which was used only in the case, where the reduced hemes should be explicitly specified. The reduction process is given at the bottom, where the fully oxidized protein was represented with four positive charges for convenience.

Table 5. The different amino acid residues around four hemes within the distance of 5 Å

Heme number in crystal	Cytochrome c_3 *Dv*MF	Cytochrome c_3 *Dv*H
Heme I	Asp (12) Lys (13)	Glu (12) Ala (13)
Heme II	Asn (42) Gln (44)	Asp (42) Arg (44)
	Ala (68) Gly (73)	Val (68) Asn (73)
Heme III	Ala(47)	Gly (47)
Heme IV	Thr (86) Glu (96)	Val (86) Asp (96)

ted from the macroscopic redox potentials and the electron-distribution probilities according to the reported procedure.[18]

The results are given in Table 4. Thirty-two microscopic redox potentials could be calculated from these values. They are shown in Figure 3.

We can find some features from the obtained microscopic redox potentials. It is clear that the redox potential of each heme is significantly changed, not only in value, but also in relative order, with the change of oxidation state. For example, heme 3 has the second highest potential in the first reduction step but becomes one with the lowest potential in the third and fourth reduction step. This strongly suggests that each heme plays a different role in the different oxidation. When the interacting potentials are compared with those of *Dv*MF,[14] it can be seen that the positive interaction is a large. And, microscopic redox potentials are very sensitive to the environment around the heme. In the case of cytochrome c_3 from *Dv*MF, the redox potential of heme 2 is the second lowest in the first reduction step, and then becomes the heme with the highest potential in the third and fourth reduction steps.[14] Cytochrome c_3 of *Dv*H very closely resembles that of *Dv*MF. They have similar isoelectric points (10.2 for *Dv*H and 10.6 for *Dv*MF) and a high sequence homology as mentioned above. However, from the three dimentional structure of cytochrome c_3 of *Dv*MF10 and *Dv*H,[11,12] we found that 9 residues out of a total of 14 different amino acid residues in the two cytochrome c_3 are in positions close to (within 5 Å) the four hemes. Table 5 shows the details.

It is concluded that the intramolecular electron exchange is very sensitive to the environment around the heme. The electron exchange rate may be regulated not only by the distance between the iron centers, but also by the arrangement of amino acids, incuding the charge distribution.[30] The change of the redox potentials of each heme was induced by interheme interactions. The remarkable feature of interacting potential in Table 4 is the high positive value of I_{23}. The high positive interaction potentials in cytochrome c_3 of *Dv*H and *Dv*MF were observed only between hemes 2 and 3. This means that the presence of an electron at heme 2 makes the reduction of heme 3 much easier. If an electrostatic interaction is the dominant contribution to an interacting potential, only a negative one would be expceted. Since hemes 2 and 3 correspond to the second and third reduction sites, this may suggest that the electron exchange mechanism in the intermediate hemes is complicated and cannot be explained by simple electrostatics. Therefore, a positive interaction should be elucidated in terms of other factors, including structural parameters. A complete explanation for this interaction requires further studies. However, one might imagine that some structural changes occur reversibly during the one-electron, four consecutive oxidation-reduction reaction of cytochrome c_3. In addition, the consideration of the relationship between molecular structure and redox potentials should be detailed.

Acknowledgment. This work was partly supported by the Korea Science and Engeering Foundation (Grant No. 941-0300-017-1), and Basic Science Research Institute, Ministry of Education (94-341). The authors are grateful to prof. H. Akutsu and K. Niki, Yokohama National University for their assistance.

References

1. Postsgate, J. R. *The Sulfate-Reducing Bacteria*; 2nd ed., Cambridge University Press: New York 1984, p 74.
2. Ishimoto, M.; Koyama, J.; Nagai, Y. *Bull. Chem. Soc. Jpn.* **1954**, *27*, 564.
3. Ishimoto, M.; Koyama, J.; Nagai, Y. *J. Biochem.(Tokyo)* **1954**, *41*, 763.
4. Ishimoto, M.; Koyama, J.; Yagi, T.; Shiraki, M. *J. Biochem. (Tokyo)* **1957**, *44*, 413.
5. Postgate, J. R. *Biochem. J.* **1954**, *56*, XI.
6. Postgate, J. R. *Biochem. J.* **1954**, *58*, IX.
7. Postgate, J. R. *J. Gen. Microbiol.* **1956**, *14*, 545.
8. Trousil, E. B.; Campbell, L. L. *J. Biol. Chem.* **1974**, *249*, 386.
9. Yagi, T.; Inoguchi, H.; Kimura, K. *Acc. Chem. Res.* **1983**, *16*, 2.
10. Higuchi, Y.; Kusunoki, M.; Matuura, Y.; Yasuoka, N.; Kakudo, M. *J. Mol. Biol.* **1984**, *172*, 109.
11. Morimoto, Y.; Tani, T.; Okumura, H.; Higuchi, Y.; Yasuoka, N. *J. Biochem.(Tokyo)* **1991**, *110*, 532.
12. Matias, P. M.; Frazao, C.; Morais, J.; Coll, M.; Carrondo, M. A. *J. Mol. Biol.* **1993**, *234*, 680.
13. Santos, H.; Moura, J. J. G.; LeGall, J.; Xavier, A. V. *Eur. J. Biochem.* **1984**, *141*, 283.
14. Fan, K.; Akutsu, H.; Kyogoku, Y.; Niki, K. *Biochemistry* **1990**, *29*, 2257.
15. Niki, K.; Kobayashi, Y.; Matsuda, H. *J. Electroanal. Chem.* **1984**, *178*, 333.
16. Brushi, M.; Loutfi, M.; Bianco, P.; Haladjian, *J. Biochem. Biophys. Res. Commun.* **1984**, *120*, 384.
17. Niki, K.; Kawasaki, Y.; Higuchi, Y.; Yasuoka, N. *Langmuir* **1987**, *3*, 982.
18. Fan, K.; Akutsu, H.; Niki, K.; Higuchi, N.; Kyogoku, Y. *J. Electroanal. Chem.* **1990**, *278*, 295.
19. Gayda, J. P.; Bertrand, P.; More, C.; Guerlesquin, F.; Bruschi, M. *Biochem. Biophys. Acta* **1985**, *829*, 262.
20. Gayda, J. P.; Yagi, T.; Benosman, H.; Bertrand, P. *FEBS Lett.* **1987**, *217*, 57.
21. Gayda, J. P.; Benosman, H.; Bertrand, P.; More, C.; Asso, M. *Eur. J. Biochem.* **1988**, *177*, 199.
22. Benosman, H.; Asso, M.; Bertrand, P.; Yagi, T.; Gayda, J. P. *Eur. J. Biochem.* **1989**, *182*, 51.
23. Park, J-S.; Kano, K.; Niki, K.; Akutsu, H. *FEBS Lett.* **1991**, *285*, 149.
24. Guigliarelli, B.; Bertrand, P.; More, C.; Haser, R.; Gayda, J. P. *J. Mol. Biol.* **1990**, *216*, 161.

25. Turner, D. L.; Salgueiro, C. A.; LeGall, J.; Xavier, A. V. *Eur. J. Biochem.* **1992**, *210*, 931.
26. Salgueiro, C. A.; Turner, D. L.; Santos, H.; LeGall, J.; Xavier, A. *FEBS Lett.* **1992**, *314*(2), 155.
27. Park, J.-S.; Kano, K.; Morimoto, Y.; Higuchi, Y.; Yasuoka, N.; Ogata, M.; Niki, K.; Akutsu, H. *J. Biomol. NMR* **1991**, *1*, 271.
28. Yagi, T.; Maruyama, K. *Biochim. Biophys. Acta* **1971**, *243*, 214.
29. Moura, J. J. G.; Santos, H.; Moura, I.; LeGall, J.; Moore, G. R.; Williams, R. J. P.; Xavier, A. V. *Eur. J. Biochem.* **1982**, *127*, 151.
30. Marcus, R. A.; Sutin, N. *Biochim. Biophys. Acta* **1985**, *811*, 265.

Preparation of Nonlinear Optical Poly(Alkyl Vinyl Ethers). 4.[1] Synthesis and Characterization of Poly[3',5'-dimethoxy-4'-(2-vinyloxyethoxy)-4-nitrostilbene] and Poly[3',5'-dimethoxy-4'-(2-vinyloxyethoxy)-2,4-dinitrostilbene]

Ju-Yeon Lee

Department of Chemistry, Inje University, Aebang-dong, Kimhae 621-749, Seoul Korea
Received December 24, 1994

3',5'-Dimethoxy-4'-(2-vinyloxyethoxy)-4-nitrostilbene **2** and 3',5'-dimethoxy-4'-(2-vinyloxyethoxy)-2,4-dinitrostilbene **5** were prepared by the reactions of 2-iodoethyl vinyl ether with 3',5'-dimethoxy-4'-hydroxy-4-nitrostilbene **1** and 3',5'-dimethoxy-4'-hydroxy-2,4-dinitrostilbene **4**, respectively. Monomers **2** and **5** were polymerized with cationic initiators to obtain polymers with 3',5'-dimethoxy-4'-oxy-4-nitrostilbene and 3',5'-dimethoxy-4'-oxy-2,4-dinitrostilbene, which are presumably effective chromophores for second-order nonlinear optical application in the side chain. The resulting polymers **3** and **6** were soluble in DMSO and DMF. The inherent viscosities of the polymers were in the range of 0.28-0.33 dL/g in DMSO. Polymers **3** and **6** showed a thermal stability up to 250 ℃ in TGA thermogram, and the T_g values obtained from DSC thermograms were in the range of 81-87°.

Introduction

Functional polymers of nonlinear optical (NLO) activity have long been the subject of curiosity and have caused recent interest.[2~6] It is well known that organic and polymeric materials with highly dipolar electronic systems exhibit NLO properties. Compared to other organic and inorganic substances, NLO polymers offer many advantages such as high nonlinear optical activity, light weight, chemical resistance, and good processability.

A potential NLO polymer must contain a highly polarizable π-electronic systems and these polymers have to be mechanically very strong. There are tremendous challenges in designing and synthesis of polymers of large NLO effects. Various polymers with the NLO-phores in the side chain such as polymethacrylates[7~13] and polystyrene[14] were reported. Polyesters,[15~19] polyurethanes,[20] polyamides,[21~22] and poly (phenyleneethynylenes)[23] containing the chromophoric main chain were also prepared. Dix etc.[24] prepared poly(ethyl vinyl ether) partly grafted with azo dyes by the reaction of poly(2-chloroethyl vinyl ether) with 4'-amino-4-nitroazobenzene. However, examples of polyalkyl vinyl ethers with the chromophoric side chain prepared directly by the polymerization of monomeric alkyl vinyl ethers are seldom found in the literature. Recently we have prepared clean poly(ethyl vinyl ethers) containing the NLO-phores *p*-oxybenzylidenemalononitrile, methyl *p*-oxybenzylidenecyanoacetate,[25] and 4'-oxy-4-nitrostilbene[26] in the side chain by cationic polymerization of the corresponding monomers.

This work is now extended with the synthesis and characterization of another poly(ethyl vinyl ethers) containing the NLO-phores 3',5'-dimethoxy-4'-oxy-4-nitrostilbene and 3',5'-dimethoxy-4'-oxy-2,4-dinitrostilbene in the side chain. The present report describes the synthesis and cationic polymerization of 3',5'-dimethoxy-4'-(2-vinyloxyethoxy)-4-nitrostilbene **2** and 3',5'-dimethoxy-4'-(2-vinyloxyethoxy)-2,4-dinitrostilbene **5**.

Experimental

Materials. 2-Chloroethyl vinyl ether, 3,5-dimethoxy-4-hydroxybenzaldehyde, *p*-nitrophenylacetic acid, piperidine, and 2,4-dinitrotoluene (Aldrich) were used as received. Sodium iodide was dried for 4 h at 100 ℃ under vacuum. Acetone was purified by drying with anhydrous potassium carbonate, followed by distillation under nitrogen. N,N-Dimethylformamide (DMF) was purified by drying with anhydrous calcium sulfate, followed by distillation under reduced pressure. Dichloromethane was washed with concentrated sulfuric acid and then with water, dried with anhydrous calcium chloride, refluxed with calcium hydride, and distilled under nitrogen before use. Toluene was washed with cold concentrated sulfuric acid and then with water, aqueous 5% sodium bicarbonate, again with water, dried with anhydrous calcium